
CobBO: Coordinate Backoff Bayesian Optimization with Two-Stage Kernels

Anonymous Author(s)

Affiliation

Address

email

Abstract

1 Bayesian optimization is a popular method for optimizing expensive black-box
2 functions. Yet it oftentimes struggles in high dimensions where the computation
3 could be prohibitively expensive and a sufficient estimation of the global landscape
4 requires more observations. We introduce Coordinate backoff Bayesian optimization
5 (CobBO) with two-stage kernels to alleviate this problem. In each iteration, a
6 promising subset of coordinates is selected in the first stage, as past observed points
7 in the full space are projected to the selected subspace adopting a simple kernel
8 that sacrifices the approximation accuracy for computational efficiency. Then in
9 the second stage of the same iteration a more sophisticated kernel is applied for
10 estimating the landscape in the selected low dimensional subspace where the com-
11 putational cost becomes affordable. Effectively, this second stage kernel refines the
12 approximation of the global landscape estimated by the first stage kernel through
13 a sequence of observations in the local subspace. This refinement lasts until a
14 stopping rule is met determining when to back off from a certain subspace and
15 switch to another coordinate subset. This decoupling significantly reduces the com-
16 putational burden in high dimensions, while the two-stage kernels of the Gaussian
17 process regressions fully leverage the observations in the whole space rather than
18 only relying on observations in each coordinate subspace. Extensive evaluations
19 show that CobBO finds solutions comparable to or better than other state-of-the-art
20 methods for dimensions ranging from tens to hundreds, while reducing the trial
21 complexity and computational costs.

22 1 Introduction

23 Bayesian optimization (BO) has emerged as an effective zero-order paradigm for optimizing expen-
24 sive black-box functions. The entire sequence of iterations rely only on the function values of the
25 already queried points without information on their derivatives. Though highly competitive in low
26 dimensions (e.g., the dimension $D \leq 20$ [15]), Bayesian optimization based on Gaussian Process
27 (GP) regression has obstacles that impede its effectiveness, especially in high dimensions.

28 **Approximation accuracy:** GP regression assumes a class of random functions in a probability space
29 as surrogates that iteratively yield posterior distributions by conditioning on the queried points. When
30 suggesting new query points, for complex functions with numerous local optima and saddle points
31 due to local fluctuations, always exactly using the values on the queried points as the conditional
32 events may mismatch the function’s local landscape by overemphasizing the approximation accuracy
33 of the global landscape.

34
35 **Curse of dimensionality:** As a sample efficient method, Bayesian optimization often suffers from
36 high dimensions. Fitting the GP model (estimating the parameters, e.g., length_scales [14]), comput-
37 ing the Gaussian process posterior and optimizing the acquisition function in high dimensions all
38

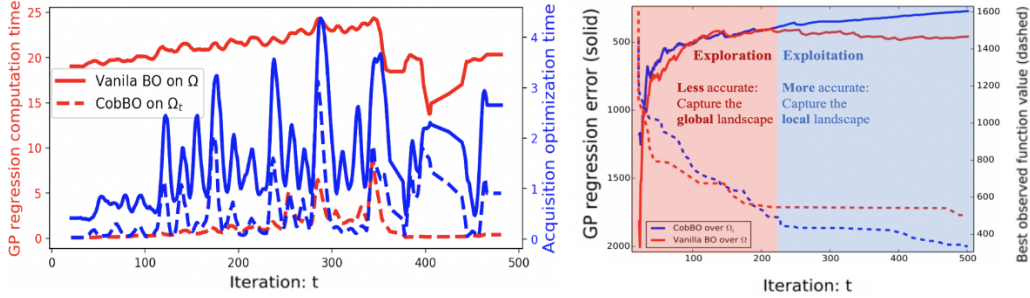


Figure 1: Minimize the fluctuated Rastrigin function on $[-5, 10]^{50}$ with 20 initial samples. [Left] Computation times for training the GP regression model and maximizing the acquisition function at each iteration. CobBO significantly reduces the execution time compared with a vanilla BO, e.g. $\times 13$ faster in this case. [Right] The average error between the GP predictions before making queries and the true function values at the queried points (solid curves, the higher the better) and the best observed function value (dashed curves, the lower the better) at iteration t . CobBO captures the global landscape less accurately using the RBF kernel, and then explores selected subspaces Ω_t more accurately using the Matern kernel. This eventually better exploits the promising subspaces.

39 incur large computational costs. It also results in statistical insufficiency of exploration [11, 65]. As
 40 the GP regression’s error grows with dimensions [8], more samples are required to balance that in
 41 high dimensions, which could cubically increase the computational costs in the worst case [45].

42 To alleviate these issues, we design coordinate backoff Bayesian optimization (CobBO) with two-
 43 stage kernels, by challenging a seemingly natural intuition stating that it is always better for Bayesian
 44 optimization to have a more accurate approximation of the objective function at all times. We
 45 demonstrate that this is not necessarily true, by showing that smoothing out local fluctuations and
 46 using the estimated function values instead of the true observations to serve as the conditional events
 47 in selected subspaces can not only significantly reduce the computation time due to the curse of
 48 dimensionality but also help in capturing the large-scale properties of the objective function $f(x)$.

49 Specifically, CobBO introduces the two-stage kernels with a stopping rule. The first stage of each
 50 iteration adopts a simple kernel that sacrifices the approximation accuracy of $f(x)$ for computational
 51 efficiency. For example, by using a universal radial basis function (RBF) approximation without
 52 learnable parameters [50], CobBO can eliminate the model fitting time in the full space. It captures
 53 a smooth approximation $\hat{f}(x)$ of the global landscape by interpolating the values of queried points
 54 projected to selected promising subspaces. These projected points serve as the conditional events
 55 for GP regression. In a selected coordinate subspace, the second stage of the same iteration applies
 56 a sophisticated kernel that can tolerate high computational cost in low dimensions. For example,
 57 CobBO uses the Automatic Relevance Determination (ARD) Matérn 5/2 kernel [40]. It refines the
 58 approximation of the local landscape by a sequence of observations determined by a stopping rule that
 59 backs off from a certain subspace and switches to another coordinate subset. In addition, computing
 60 the Gaussian process posterior and optimizing the acquisition function are both efficiently conducted
 61 in the low dimensional subspaces, bypassing the curse of dimensionality.

62 For iteration t , instead of directly computing the Gaussian process posterior distribution
 63 $\{\hat{f}(x) | \mathcal{H}_t = \{(x_i, y_i)\}_{i=1}^t, x \in \Omega\}$ by conditioning on the observations $y_i = f(x_i)$ at queried
 64 points x_i in the full space $\Omega \subset \mathbb{R}^D$ for $i = 1, \dots, t$, we change the conditional events, and consider

$$\{\hat{f}(x) | R(P_{\Omega_t}(x_1, \dots, x_t), \mathcal{H}_t), x \in \Omega_t, \Omega_t \subset \Omega\}$$

65 for a projection function $P_{\Omega_t}(\cdot)$ to a random subspace Ω_t and an interpolation function $R(\cdot, \cdot)$, e.g.,
 66 using a RBF approximation without learnable parameters [50] as the simple kernel for the first
 67 stage. The projection $P_{\Omega_t}(\cdot)$ maps the queried points to virtual points on a subspace Ω_t of a lower
 68 dimension [51]. The interpolation function $R(\cdot, \cdot)$ estimates the objective values at the virtual points
 69 using the queried points and their values as specified by \mathcal{H}_t . The second stage within the subspace Ω_t
 70 uses the more sophisticated kernel, e.g., Matérn 5/2 kernel [40], which has a number of parameters
 71 that otherwise would be expensive to be learned in high dimensions.

72 This method can be viewed as a variant of block coordinate ascent tailored to Bayesian optimization by
73 applying backoff stopping rules for switching coordinate blocks. While similar work exists [43, 48],
74 CobBO differs by introducing the two-stage kernels and addressing the following three issues:

- 75 1. Selecting a block of coordinates for ascending requires determining the block size as well as
76 the coordinates therein. CobBO selects the coordinate subsets by a multiplicative weights
77 update method [2] to the preference probability associated with each coordinate. Thus, it
78 samples more promising subspaces with higher probabilities.
- 79 2. A coordinate subspace requires a sufficient number of query points acting as the conditional
80 events for the GP regression. CobBO leverages all observations in the whole space by
81 interpolating the values of queried points projected to selected promising subspaces, rather
82 than simply starting from scratch in each subspace.
- 83 3. Querying a certain subspace, under some trial budget, comes at the expense of exploring
84 other coordinate blocks. Yet prematurely shifting to different subspaces does not fully
85 exploit the full potential of a given subspace. Hence determining the number of consecutive
86 function queries within a subspace makes a trade-off between exploration and exploitation.
87 CobBO uses a stopping rule in each subspace to switch the selected coordinates. When
88 consecutively querying data points in the same subspace, CobBO does not need to conduct
89 the first-stage function approximation in the full space, which is far more efficient.

90 Through comprehensive evaluations, CobBO demonstrates appealing performance for dimensions
91 ranging from tens to hundreds. It obtains comparable or better solutions with fewer queries, in
92 comparison with the state-of-the-art methods, for most of the problems tested in Section 4.2.

93 2 Related work

94 Certain assumptions are often imposed on the latent structure in high dimensions. Typical assumptions
95 include low dimensional structures and additive structures. Their advantages manifest on problems
96 with a low dimension or a low effective dimension. However, these assumptions do not necessarily
97 hold for non-separable functions with no redundant dimensions.

98 *Low dimensional structure:* The black-box function f is assumed to have a low effective dimen-
99 sion [30, 58], e.g., $f(x) = g(\Phi x)$ with some function $g(\cdot)$ and a matrix Φ of $d \times D$, $d \ll D$. A
100 number of different methods have been developed, including random embedding [66, 11, 63, 36,
101 44, 70, 5, 32], low-rank matrix recovery [11, 58], and learning subspaces by derivative informa-
102 tion [11, 13]. In contrast to existing work on subspace selections, e.g., Hashing-enhanced Subspace
103 BO (HeSBO) [44], Mahalanobis kernel for linear embeddings [33], DROPOUT [35] and LineBO [29]
104 (which receives a special treatment in Appendix F), CobBO efficiently leverages all the observations
105 in the whole space using the two-stage kernels and the stopping rule in each subspace for consecutive
106 observations, rather than only relying on limited observations in each coordinate subspace. It exploits
107 subspace structure from a perspective of block coordinate ascent, independent of the dimensions,
108 different from some algorithms that are more suitable for low dimensions, e.g., BADS [1].

109 *Additive structure:* A decomposition assumption is often made by $f(x) = \sum_{i=1}^k f^{(i)}(x_i)$, with x_i
110 defined over low-dimensional components. In this case, the effective dimensionality of the model is
111 the largest dimension among all additive groups [45], which is usually small. The Gaussian process
112 is structured as an additive model [17, 28], e.g., projected-additive functions [36], ensemble Bayesian
113 optimization (EBO) [61], latent additive structural kernel learning (HDBBO) [65] and group additive
114 models [28, 36]. However, learning the unknown structure incurs a considerable computational
115 cost [44], and is not applicable for non-separable functions, for which CobBO can still be applied.

116 *Trust regions and space partitions:* Trust region BO has been proven effective for high-dimensional
117 problems. A typical pattern is to alternate between global and local search regions. In the local
118 trust regions, many efficient methods have been applied, e.g., local Gaussian models (TurBO [14]),
119 adaptive search on a mesh grid (BADS [1]) or quasi-Newton local optimization (BLOSSOM [41]).
120 TurBO [14] uses Thompson sampling to allocate samples across multiple regions. A related method is
121 to use space partitions, e.g., LA-MCTS[60] on a Monte Carlo tree search algorithm to learn efficient
122 partitions. CobBO differs by selecting low dimensional subspaces. It can also incorporate trust
123 regions in the first-stage global approximation, as shown in the Appendix.

124 3 Algorithm

125 Without loss of generality, suppose that the goal is to solve a maximization problem $x^* =$
 126 $\operatorname{argmax}_{x \in \Omega} f(x)$ for a black-box function $f : \Omega \rightarrow \mathbb{R}$. The domain is normalized $\Omega = [0, 1]^D$
 127 with the coordinates indexed by $I = \{1, 2, \dots, D\}$.

128 For a sequence of points $\mathcal{X}_t = \{x_1, x_2, \dots, x_t\}$ with t indexing the most recent iteration, we observe
 129 $\mathcal{H}_t = \{(x_i, y_i = f(x_i))\}_{i=1}^t$. A random subset $C_t \subseteq I$ of the coordinates is selected, forming a
 130 subspace $\Omega_t \subseteq \Omega$ at iteration t . As a variant of coordinate ascent, the subspace Ω_t contains a pivot
 131 point V_t , which presumably is the maximum point $x_t^M = \operatorname{argmax}_{x \in \mathcal{X}_t} f(x)$ with $M_t = f(x_t^M)$.
 132 CobBO may set V_t different from x_t^M to escape local optima. Then, BO is conducted within Ω_t while
 133 fixing all the other coordinates $C_t^c = I \setminus C_t$, i.e., the complement of C_t .

Algorithm 1: CobBO(f, τ, T)

```

1  $\mathcal{H}_\tau \leftarrow$  sample  $\tau$  initial points and evaluate their values
2  $V_\tau, M_\tau \leftarrow$  Find the tuple with the maximal objective value in  $\mathcal{H}_\tau$ 
3  $q_\tau \leftarrow 0$  Initialize the number of consecutive failed queries
4  $\pi_\tau \leftarrow$  Initialize a uniform preference distribution on the coordinates
5 for  $t \leftarrow \tau$  to  $T$  do
6   if switch  $\Omega_{t-1}$  by the backoff stopping rule (Section 3.2) then
7      $C_t \leftarrow$  Sample a promising coordinate block according to  $\pi_t$  (Section 3.1)
8      $\Omega_t \leftarrow$  Take the subspace of  $\Omega_t$  over the coordinate block  $C_t$ , such that  $V_t \in \Omega_t$ 
9   else
10     $\Omega_t \leftarrow \Omega_{t-1}$ 
11     $\hat{\mathcal{X}}_t \leftarrow P_{\Omega_t}(\mathcal{X}_t)$  [Project  $\mathcal{X}_t$  onto  $\Omega_t$  to obtain a set of virtual points (Eq. 1)]
12     $\hat{\mathcal{H}}_t \leftarrow R(\hat{\mathcal{X}}_t, \mathcal{H}_t)$  [Smooth function values on  $\hat{\mathcal{X}}_t$  by interpolation using  $\mathcal{H}_t$ ]
13     $p[\hat{f}_{\Omega_t}(x)|\hat{\mathcal{H}}_t] \leftarrow$  Compute the posterior distribution of the Gaussian process in  $\Omega_t$ 
      conditional on  $\hat{\mathcal{H}}_t$ 
14     $x_{t+1} \leftarrow \operatorname{argmax}_{x \in \Omega_t} Q_{\hat{f} \sim p(\hat{f}|\hat{\mathcal{H}}_t)}(x|\hat{\mathcal{H}}_t)$  [Suggest the next query in  $\Omega_t$  (Section 3)]
15     $y_{t+1} \leftarrow$  Evaluate the black-box function  $y_{t+1} = f(x_{t+1})$ 
16    if  $y_{t+1} > M_t$  then
17       $V_{t+1} \leftarrow x_{t+1}, M_{t+1} \leftarrow y_{t+1}, q_{t+1} \leftarrow 0$ 
18    else
19       $V_{t+1} \leftarrow V_t, M_{t+1} \leftarrow M_t, q_{t+1} \leftarrow q_t + 1$ 
20     $\pi_{t+1} \leftarrow$  Update  $\pi_t$  by a multiplicative weights update method (Eq. 2)
21     $\mathcal{H}_{t+1} \leftarrow \mathcal{H}_t \cup \{(x_{t+1}, y_{t+1})\}, \mathcal{X}_{t+1} \leftarrow \mathcal{X}_t \cup \{x_{t+1}\}$ 
22 end

```

134 For BO in Ω_t , we use Gaussian processes as the random surrogates $\hat{f} = \hat{f}_{\Omega_t}(x)$ to describe the
 135 Bayesian statistics of $f(x)$ for $x \in \Omega_t$. At each iteration, the next query point is generated by solving

$$x_{t+1} = \operatorname{argmax}_{x \in \Omega_t, V_t \in \Omega_t} Q_{\hat{f}_{\Omega_t}(x) \sim p(\hat{f}|\mathcal{H}_t)}(x|\mathcal{H}_t),$$

136 where the acquisition function $Q(x|\mathcal{H}_t)$ incorporates the posterior distribution of the Gaussian
 137 processes $p(\hat{f}|\mathcal{H}_t)$. Typical acquisition functions include the expected improvement (EI) [42, 27],
 138 the upper confidence bound (UCB) [3, 54, 55], the entropy search [24, 25, 64], and the knowledge
 139 gradient [16, 53, 69].

140 Instead of directly computing the posterior distribution $p(\hat{f}|\mathcal{H}_t)$, we replace the conditional events
 141 \mathcal{H}_t by

$$\hat{\mathcal{H}}_t := R(P_{\Omega_t}(\mathcal{X}_t), \mathcal{H}_t) = \{(\hat{x}_i, \hat{y}_i)\}_{i=1}^t$$

142 with an interpolation function $R(\cdot, \cdot)$ and a projection function $P_{\Omega_t}(\cdot)$,

$$P_{\Omega_t}(x)^{(j)} = \begin{cases} x^{(j)} & \text{if } j \in C_t \\ V_t^{(j)} & \text{if } j \notin C_t \end{cases} \quad (1)$$

143 at coordinate j . It simply keeps the values of x whose corresponding coordinates are in C_t and
 144 replaces the rest by the corresponding values of V_t , as illustrated in Fig. 2.

145 Applying $P_{\Omega_t}(\cdot)$ on \mathcal{X}_t and discarding duplicates generate a new set of distinct virtual points $\hat{\mathcal{X}}_t =$
 146 $\{\hat{x}_1, \hat{x}_2, \hat{x}_3, \dots, \hat{x}_{\hat{t}}\}$, $\hat{x}_i \in \Omega_t \forall 1 \leq i \leq \hat{t} \leq t$. The function values at $\hat{x}_i \in \hat{\mathcal{X}}_t$ are interpolated as
 147 $\hat{y}_i = R(\hat{x}_i, \mathcal{H}_t)$ using the standard radial basis function [6, 7] and the observed points in \mathcal{H}_t . It not
 148 only significantly reduces the GP regression time due to the efficiency of RBF [6] and the acquisition
 149 function optimization in low dimensions [11], but also eventually improves the model accuracy using
 150 the more sophisticated kernel applied on Ω_t .

151 Note that only a fraction of the points in $\hat{\mathcal{X}}_t \cap \mathcal{X}_t$
 152 directly observe the exact function values. The
 153 function values on the rest ones in $\hat{\mathcal{X}}_t \setminus \mathcal{X}_t$ are
 154 estimated by interpolation, which captures the
 155 landscape of $f(x)$ by smoothing out the local
 156 fluctuations. To control the trade-off between
 157 the inaccurate estimations and the exact observa-
 158 tions in Ω_t , we design a stopping rule that
 159 optimizes the number of consistent queries in
 160 Ω_t . The more consistent queries conducted in a
 161 given subspace, the more accurate observations
 162 could be obtained, albeit at the expense of a smaller remaining budget for exploring other regions.

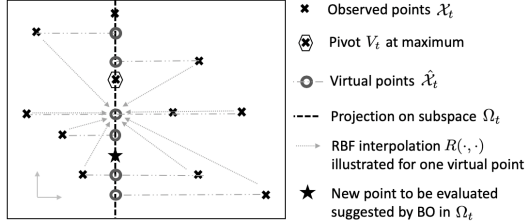


Figure 2: Two-stage kernels: subspace projection and function value interpolation

163 The key features of CobBO are listed in Algorithm 1, with more details in the following sections.
 164 Several auxiliary components are utilized and presented in Appendix C to deal with a larger variety
 165 of problems and corner cases.

166 3.1 Block coordinate ascent and subspace selection

167 For Bayesian optimization, consider an infeasible assumption that each iteration can exactly maximize
 168 the function $f(x)$ in Ω_t . This is not possible for one iteration but only if one can consistently query
 169 in Ω_t , since the points converge to the maximum, e.g., under the expected improvement acquisition
 170 function with fixed priors [59] and the convergence rate can be characterized for smooth functions
 171 in the reproducing kernel Hilbert space [8]. However, even with this infeasible assumption, it is
 172 known that coordinate ascent with fixed blocks can cause stagnation at a non-critical point, e.g., for
 173 non-differentiable [67] or non-convex functions [49]. This motivates us to select a subspace with a
 174 variable-size coordinate block C_t for each query. A good coordinate block can help the iterations
 175 to escape the trapped non-critical points. For example, one condition can be based on the result
 176 in [21] that assumes $f(x)$ to be differentiable and strictly quasi-convex over a collection of blocks. In
 177 practice, we do not restrict ourselves to these assumptions.

178 We induce a preference distribution π_t over the coordinate set I , and sample a variable-size coordinate
 179 block C_t accordingly. This distribution is updated at iteration t through a multiplicative weights
 180 update method [2]. Specifically, the values of π_t at coordinates in C_t starts off uniform and increase
 181 in face of an improvement or decrease otherwise according to different multiplicative ratios $\alpha > 1$
 182 and $\beta > 1$, respectively,

$$w_{t,j} = w_{t-1,j} \cdot \begin{cases} \alpha & \text{if } j \in C_t \text{ and } y_t > M_{t-1} \\ 1/\beta & \text{if } j \in C_t \text{ and } y_t \leq M_{t-1} \\ 1 & \text{if } j \notin C_t \end{cases} ; \quad w_{0,j} = \frac{1}{D} ; \quad \pi_{t,j} = \frac{w_{t,j}}{\sum_{j=1}^D w_{t,j}} \quad (2)$$

183 This update characterizes how likely a coordinate block can generate a promising search subspace.
 184 The multiplicative ratio α is chosen to be relatively large, e.g., $\alpha = 2.0$, and β relatively small, e.g.,
 185 $\beta = 1.1$, since the queries that improve the best observations $y_t > M_{t-1}$ happen more rarely than
 186 the opposite $y_t \leq M_{t-1}$.

187 How to dynamically select the size $|C_t|$? It is known that Bayesian optimization works well for low
 188 dimensions [15]. Thus, we specify an upper bound for the dimension of the subspace (e.g. $|C_t| \leq 30$).
 189 In principle, $|C_t|$ can be any random number in a finite set of possible block sizes \mathcal{C} . This is different
 190 from the method that partitions the coordinates into fixed blocks and selects one according to, e.g.,
 191 cyclic order [68], random sampling or Gauss-Southwell [46].

192 3.2 Backoff stopping rule for consistent queries

193 Applying BO on Ω_t requires a strategy to determine the number of consecutive queries for making a
 194 sufficient progress. This strategy is based on previous observations, thus forming a stopping rule. In
 195 principle, there are two different scenarios, exemplifying exploration and exploitation, respectively.
 196 Persistently querying a given subspace refrains from opportunistically exploring other coordinate
 197 combinations. Abruptly shifting to different subspaces does not fully exploit the potential of a given
 198 subspace.

199 CobBO designs a heuristic stopping rule in compromise. It takes the above two scenarios into
 200 job consideration, by considering not only the number of consecutive queries that fail to improve
 201 the objective function but also other factors including the improved difference $M_t - M_{t-1}$, the
 202 point distance $\|x_t - x_{t-1}\|$, the query budget T and the problem dimension D . On the one hand,
 203 switching to another subspace $\Omega_{t+1} (\neq \Omega_t)$ prematurely without fully exploiting Ω_t incurs an
 204 additional approximation error associated with the interpolation of observations in Ω_t projected to
 205 Ω_{t+1} . On the other hand, it is also possible to over-exploit a subspace, spending high query budget
 206 on marginal improvements around local optima. In order to mitigate this, even when a query leads to
 207 an improvement, other factors are considered for sampling a new subspace.

208 3.3 Theoretical Analysis

209 One can view our block coordinate selection approach in section 3.1 as a combinatorial mixture of
 210 experts problem [10], where each coordinate is a single expert and the forecaster aims at choosing
 211 the best combination of experts in each step. Under this view, we bound the regret of our selection
 212 method with respect to the policy of selecting the best (unknown) block of coordinates at each step.

213 Assume that there is a fixed optimal choice \mathcal{I}^* for the block of coordinates to pick at all steps. This
 214 block is characterized by improving the objective function for the largest number of times among
 215 all the possible coordinate blocks when performing Bayesian optimization over the corresponding
 216 subspaces. The following particular design of losses expresses this cause:

$$\ell_{t,i} = \begin{cases} -\log(\tilde{\alpha}) & \text{if } i \in C_t \text{ and } y_t > M_{t-1} \\ \log(\tilde{\beta}) & \text{if } i \in C_t \text{ and } y_t \leq M_{t-1} \\ 0 & \text{if } i \notin C_t \end{cases} \quad ; \quad \tilde{\alpha}, \tilde{\beta} > 1 \quad (3)$$

217 as all the coordinates participating in the selected block incur the same loss that effectively rewards
 218 these coordinates for improving the objective and penalizes these for failing to improve the objective.
 219 All other coordinates that are not selected receive a zero loss and remain untouched.

220 Note that $\tilde{\alpha}$ and $\tilde{\beta}$ express the extent of reward and penalty, e.g. for $\tilde{\alpha} = \tilde{\beta} = e$ we have losses of
 221 $\ell_{t,i} \in \{-1, 1, 0\}$. Yet, $\tilde{\alpha}$ is better chosen to be larger than $\tilde{\beta}$, since the frequency of improving the
 222 objective is expected to be smaller.

223 The loss received by the forecaster is to reflect the same motivation. This is done by averaging
 224 the losses of the individual coordinates in the selected block, so that the size of the block does not
 225 matter explicitly, i.e. a bigger block should not incur more loss just due to its size but only due to its
 226 performance. Such that for each coordinate block $\mathcal{I}_t \subset \mathcal{I} = \{1, \dots, D\}$ selected at time step t , the
 227 loss incurred by the forecaster is $L_{t,\mathcal{I}_t} = \frac{1}{|\mathcal{I}_t|} \sum_{i \in \mathcal{I}_t} \ell_{t,i}$. This is also the common loss incurred by
 228 all the coordinates participating in that block.

229 In each step we have the following multiplicative update rule of the weights associated with each
 230 coordinate (setting $\alpha = \tilde{\alpha}^\eta$ and $\beta = \tilde{\beta}^\eta$ yields the update rule in Eq. 2):

$$w_{t,i} = w_{t-1,i} \cdot e^{-\eta \ell_{t,i}} = w_{t-1,i} \cdot \begin{cases} \tilde{\alpha}^\eta & \text{if } i \in C_t \text{ and } y_t > M_{t-1} \\ 1/\tilde{\beta}^\eta & \text{if } i \in C_t \text{ and } y_t \leq M_{t-1} \\ 1 & \text{if } i \notin C_t \end{cases} \quad (4)$$

The probability $\tilde{\pi}_{t,\mathcal{I}_t}$ of selecting a certain coordinate block \mathcal{I}_t is induced by π_t as specified next.
 Thus the expected cumulative loss of the forecaster is:

$$L_T = \sum_{t=1}^T \sum_{c \in \mathcal{C}} \sum_{\mathcal{I}_t \in \mathcal{S}_c} \tilde{\pi}_{t,\mathcal{I}_t} \cdot \frac{1}{|\mathcal{I}_t|} \sum_{i \in \mathcal{I}_t} \ell_{t,i}$$

Assume the best coordinate block is \mathcal{I}^* , then the corresponding cumulative loss is:

$$L_T^* = \sum_{t=1}^T L_{t, \mathcal{I}^*} = \sum_{t=1}^T \frac{1}{|\mathcal{I}^*|} \sum_{i \in \mathcal{I}^*} \ell_{t,i}$$

231 We hence aim at bounding the regret $\text{Regret}_T = L_T - L_T^*$.

232 **Theorem 1.** *Sample from the combinatorial space of all possible coordinate blocks $\mathcal{I}_t \in \bigcup_{c \in \mathcal{C}} \mathcal{S}_c$*
 233 *with probability $\tilde{\pi}_{t, \mathcal{I}_t} = \prod_{i \in \mathcal{I}_t} \tilde{w}_{t, \mathcal{I}_t} / \sum_{c \in \mathcal{C}} \sum_{\hat{\mathcal{I}} \in \mathcal{S}_c} \prod_{j \in \hat{\mathcal{I}}} \tilde{w}_{t, \hat{\mathcal{I}}}$. Then the update rule in Eq. 2 with*
 234 *$\alpha = \tilde{\alpha}^\eta$, $\beta = \tilde{\beta}^\eta$ and $\eta = \log(\tilde{\alpha}\tilde{\beta})^{-1} \sqrt{T^{-1}|\mathcal{C}|D \log(D)}$ yields:*

$$\text{Regret}_t \leq \mathcal{O} \left((\log(\tilde{\alpha}\tilde{\beta}) \cdot \sqrt{T|\mathcal{C}|D \log(D)}) \right) \quad (5)$$

235 where $\tilde{w}_{t, \mathcal{I}_t} = \prod_{i \in \mathcal{I}_t} w_{t,i}^{1/|\mathcal{I}_t|}$ is the geometric mean of weights in block \mathcal{I}_t . The upper bound in Eq. 5
 236 is tight, as the lower bound can be shown to be of $\Omega(\sqrt{T \log(N)})$ [23] where the number of experts
 237 is $N = \sum_{c \in \mathcal{C}} \mathcal{S}_c \leq D^{|\mathcal{C}|D}$ in our combinatorial setup, as typically $|\mathcal{C}| \ll D$.

238 In practice, the direct sampling policy introduced in Theorem 1 involves high computational costs due
 239 to the exponential growth of combinations in D . Thus CobBO suggests an alternative computationally
 240 efficient sampling policy with a linear growth in D .

241 **Theorem 2.** *Sample a block size $c \in \mathcal{C}$ with probability p_c and c coordinates without replacement*
 242 *according to π_t . Assume $\mathcal{C} \supset \{1\}$, then the update rule in Eq. 2, with $\alpha = \tilde{\alpha}^\eta$, $\beta = \tilde{\beta}^\eta$ and*
 243 *$\eta = \sqrt{\frac{\log(D)}{T(\log(\tilde{\alpha}\tilde{\beta})^2 - \log(p_1))}} \geq 1$ yields:*

$$\text{Regret}_t \leq \mathcal{O} \left(\sqrt{(\log(\tilde{\alpha}\tilde{\beta})^2 - \log(p_1)) \cdot \sqrt{T \log(D)}} \right) \quad (6)$$

244 where $p_c > 0$ for all $c \in \mathcal{C}$ and $\sum_{c \in \mathcal{C}} p_c = 1$, e.g., uniformly set $p_c \equiv |\mathcal{C}|^{-1}$. The proof and detailed
 245 sampling policy are in Appendix A. The regret upper bound in Eq. 6 is tight, as the lower bound for
 246 an easier setup can be shown to be of $\Omega(\sqrt{T \log(D)})$ [23]. The implication on η is valid only for
 247 settings of a very high dimensionality and low query budget. In particular, CobBO is designed for
 248 this kind of problems.

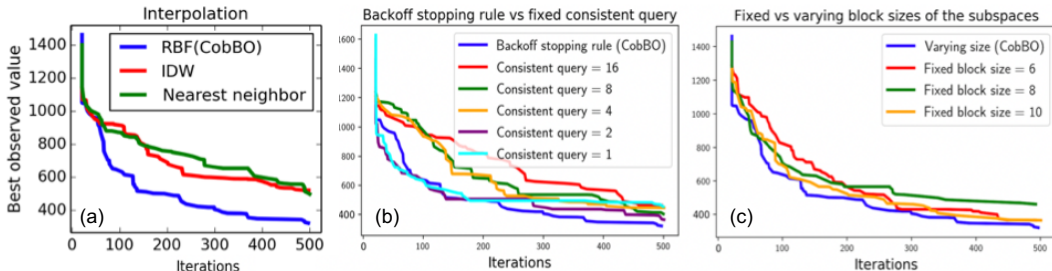
249 **Remark:** Similar analysis and results follow when incorporating consistent queries from Section 3.2
 250 and sampling a new coordinate block once every several steps. This is done by effectively performing
 251 less steps of aggregated temporal losses, as shown in Appendix A.

252 4 Numerical Experiments

253 This section presents detailed ablation studies of the key components presented in Section 3 and
 254 comparisons with other algorithms.

255 4.1 Empirical analysis and ablation study

256 Ablation studies are designed to study the contributions of the key components in Algorithm 1 by
 257 experimenting with the Rastrigin function on $[-5, 10]^{50}$ with 20 initial points. The best performing
 run out of 5 experiments for each configuration is presented in Figure 3.



258 Figure 3: Ablation study using Rastrigin on $[-5, 10]^{50}$ with 20 initial random samples

259 **RBF interpolation:** RBF calculation is time efficient. Specifically, this is much beneficial in high
 260 dimensions. Figure 1 (left) shows the computation time of plain Bayesian optimization compared to
 261 CobBO’s. While the former applies GP regression using the Matérn kernel in the high dimensional
 262 space directly, the later applies RBF interpolation in the high dimensional space and GP regression
 263 with the Matérn kernel in the low dimensional subspace. This two-step composite kernel leads to a
 264 significant speed-up. Other time efficient alternatives are, e.g., the inverse distance weighting [26]
 265 and the simple approach of assigning the value of the observed nearest neighbour. Figure 3 (a) shows
 266 that RBF is the most favorable.

267 **Backoff stopping rule:** CobBO applies a stopping rule to query a variable number of points in
 268 subspace Ω_t (Section 3.2). To validate its effectiveness, we compare it with schemes that use a fixed
 269 budget of queries for Ω_t . Figure 3 (b) shows that the stopping rule yields superior results.

270 **Coordinate blocks of a varying size:** CobBO selects a block of coordinates of a varying size C_t
 271 (Section 3.1). Figure 3 (c) shows that a varying size is better than fixed.

272 **Preference probability over coordinates:** For
 273 demonstrating the effectiveness of coordinate
 274 selection (Section 3.1), we artificially let the
 275 function value only depend on the first 25 coordi-
 276 nates of its input and ignore the rest. It forms
 277 two separate sets of active and inactive coordi-
 278 nates, respectively. We expect CobBO to refrain
 279 from selecting inactive coordinates. Figure 4
 280 shows the entropy of this preference probability
 281 π_t over coordinates and the overall probability
 282 for picking active and inactive coordinate at each
 283 iteration. We see that the entropy decreases, as
 284 the preference distribution concentrates on the
 285 significant active coordinates.

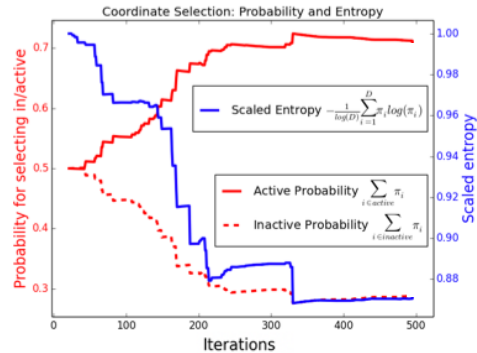


Figure 4: The preference probability focuses on active coordinates as the entropy decreases

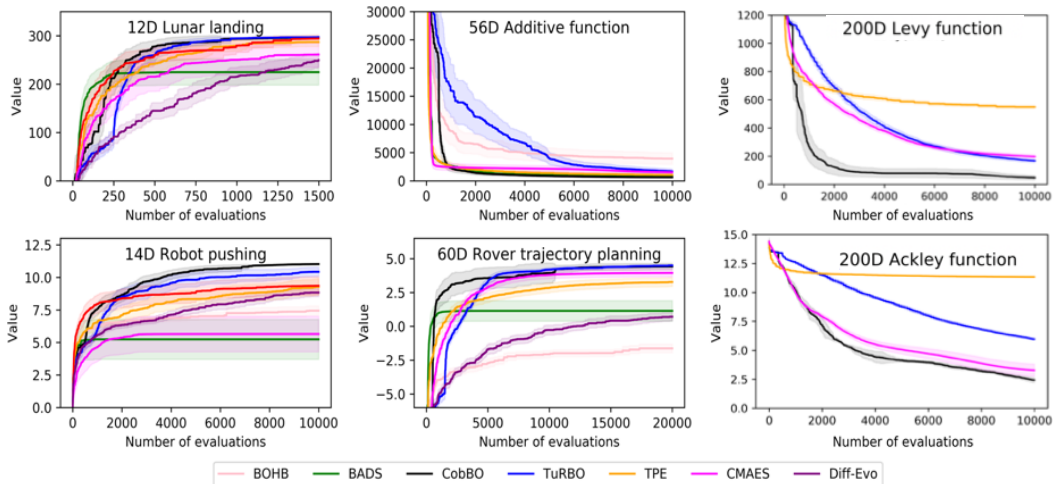


Figure 5: Performance over low (left) medium (middle) and high (right) dimensional problems

286 4.2 Comparisons with other methods

287 The default configuration for CobBO is specified in the supplementary materials. CobBO performs
 288 on par or outperforms a collection of state-of-the-art methods across the following experiments. Most
 289 of the experiments are conducted using the same settings as in Turbo [14], where it is compared
 290 with a comprehensive list of baselines, including BFGS, BOCK [47], BOHAMIANN, CMA-ES [22],
 291 BOBYQA, EBO [61], GP-TS, HeSBO [44], Nelder-Mead and random search. To avoid repetitions,
 292 we only show Turbo and CMA-ES that achieve the best performance among this list, and additionally
 293 compare CobBO with BADS [1], REMBO [63], Differential Evolution (Diff-Evo) [56], Tree Parzen
 294 Estimator (TPE) [4] and Adaptive TPE (ATPE) [12].

295 **4.2.1 Low dimensional tests**

296 To evaluate CobBO on low dimensional problems, we use the lunar landing [38, 14] and robot
297 pushing [62], by following the setup in [14]. Confidence intervals (95%) over 30 independent
298 experiments for each problem are shown in Fig. 5.

299 **Lunar landing (maximization):** This controller learning problem (12 dimensions) is provided by
300 the OpenAI gym [38] and evaluated in [14]. Each algorithm has 50 initial points and a budget of
301 1, 500 trials. TuRBO is configured with 5 trust regions and a batch size of 50 as in [14]. Fig. 5 (upper
302 left) shows that, among the 30 independent tests, CobBO quickly exceeds 300 along some good
303 sample paths.

304 **Robot pushing (maximization):** This control problem (14 dimensions) is introduced in [62] and
305 extensively tested in [14]. We follow the setting in [14], where TuRBO is configured with a batch
306 size of 50 and 15 trust regions, each of which has 30 initial points. Each experiment has a budget of
307 10, 000 evaluations. On average CobBO exceeds 10 within 5500 trials, as shown in Fig. 5 (lower
308 left).

309 **4.2.2 High dimensional tests**

310 Since the duration of each experiment in this section is long, confidence intervals (95%) over repeated
311 10 independent experiments for each problem are presented.

312 **Additive latent structure (minimization):** As mentioned in Section 2, additive latent structures
313 have been exploited in high dimensions. We construct an additive function of 56 dimensions, defined
314 as $f_{56}(x) = \text{Ackley}(x_1) + \text{Levy}(x_2) + \text{Rastrigin}(x_3) + \text{Hartmann}(x_4) + \text{Rosenbrock}(x_5) +$
315 $\text{Schwefel}(x_6)$, where the first three terms express the exact functions and domains described in
316 Section 4.2.1, the Hartmann function on $[0, 1]^6$ and the Rosenbrock and Schwefel functions on
317 $[-5, 10]^{10}$ and $[-500, 500]^{10}$, respectively.

318 We compare CobBO with TPE, BADS, CMA-ES and TuRBO, each with 100 initial points. Specifi-
319 cally, TuRBO is configured with 15 trust regions and a batch size 100. ATPE is excluded as it takes
320 more than 24 hours per run to finish. The results are shown in Fig. 5 (upper middle), where CobBO
321 quickly finds the best solution among the algorithms tested.

322 **Rover trajectory planning (maximization):** This problem (60 dimensions) is introduced in [62].
323 The objective is to find a collision-avoiding trajectory of a sequence consisting of 30 positions in a
324 2-D plane. We compare CobBO with TuRBO, TPE and CMA-ES, each with a budget of 20, 000
325 evaluations and 200 initial points. TuRBO is configured with 15 trust regions and a batch size of
326 100, as in [14]. ATPE, BADS and REMBO are excluded for this problem and the following ones,
327 as they all take more than 24 hours per run. Fig. 5 (lower middle) shows that CobBO has a good
328 performance.

329 **The 200-dimensional Levy and Ackley functions (minimization):** We minimize the Levy and
330 Ackley functions over $[-5, 10]^{200}$ with 500 initial points. TuRBO is configured with 15 trust regions
331 and a batch size of 100. These two problems are challenging and have no redundant dimensions. For
332 Levy, in Fig. 5 (upper right), CobBO reaches 100.0 within 2, 000 trials, while CMA-ES and TuRBO
333 obtain 200.0 after 8, 000 trials. TPE cannot find a comparable solution within 10, 000 trials in this
334 case. For Ackley, in Fig. 5 (lower right), CobBO reaches the best solution among all of the algorithms
335 tested.

336 Regarding running times, for Ackley, CobBO runs for 12.8 CPU hours and TuRBO-1 run for more
337 than 80 CPU hours or 9.6 GPU hours. Most other methods either cannot make any progress or find
338 far worse solutions.

339 **5 Conclusion**

340 CobBO is a variant of coordinate ascent tailored for Bayesian optimization with a stopping rule to
341 switch coordinate subspaces. The sampling policy of subspaces is proven to have tight regret bounds
342 with respect to the best subspace in hindsight. Combining this projection on random subspaces with a
343 two-stage kernels for function value interpolation and GP regression, we provide a practical Bayesian
344 optimization method of affordable computational costs in high dimensions. Empirically, CobBO
345 consistently finds comparable or better solutions with reduced trial complexity in comparison with
346 the state-of-the-art methods across a variety of benchmarks.

347 **References**

- 348 [1] Luigi Acerbi and Wei Ji Ma. Practical bayesian optimization for model fitting with bayesian
 349 adaptive direct search. In *Proceedings of the 31st International Conference on Neural Infor-*
 350 *mation Processing Systems*, NIPS'17, page 1834–1844, Red Hook, NY, USA, 2017. Curran
 351 Associates Inc.
- 352 [2] Sanjeev Arora, Elad Hazan, and Satyen Kale. The multiplicative weights update method: a
 353 meta-algorithm and applications. *Theory of Computing*, 8(6):121–164, 2012.
- 354 [3] Peter Auer. Using confidence bounds for exploitation-exploration trade-offs. *J. Mach. Learn.*
 355 *Res.*, 3(null):397–422, Mar. 2003.
- 356 [4] James S. Bergstra, Rémi Bardenet, Yoshua Bengio, and Balázs Kégl. Algorithms for hyper-
 357 parameter optimization. In J. Shawe-Taylor, R. S. Zemel, P. L. Bartlett, F. Pereira, and K. Q.
 358 Weinberger, editors, *Advances in Neural Information Processing Systems 24*, pages 2546–2554.
 359 Curran Associates, Inc., 2011.
- 360 [5] Mickaël Binois, David Ginsbourger, and Olivier Roustant. On the choice of the low-dimensional
 361 domain for global optimization via random embeddings. *Journal of Global Optimization*,
 362 76(1):69–90, January 2020.
- 363 [6] Martin D. Buhmann. *Radial Basis Functions: Theory and Implementations*. Cambridge
 364 Monographs on Applied and Computational Mathematics. Cambridge University Press, 2003.
- 365 [7] Martin D. Buhmann and M. D. Buhmann. *Radial Basis Functions*. Cambridge University Press,
 366 USA, 2003.
- 367 [8] Adam D. Bull. Convergence rates of efficient global optimization algorithms. *Journal of*
 368 *Machine Learning Research*, 12(88):2879–2904, 2011.
- 369 [9] Roberto Calandra, André Seyfarth, Jan Peters, and Marc Peter Deisenroth. Bayesian optimiza-
 370 tion for learning gaits under uncertainty. *Annals of Mathematics and Artificial Intelligence*,
 371 76(1):5–23, 2016.
- 372 [10] Nicolo Cesa-Bianchi and Gábor Lugosi. *Prediction, learning, and games*. Cambridge university
 373 press, 2006.
- 374 [11] Josip Djolonga, Andreas Krause, and Volkan Cevher. High-dimensional gaussian process
 375 bandits. In C. J. C. Burges, L. Bottou, M. Welling, Z. Ghahramani, and K. Q. Weinberger,
 376 editors, *Advances in Neural Information Processing Systems 26*, pages 1025–1033. Curran
 377 Associates, Inc., 2013.
- 378 [12] ElectricBrain. Blog: Learning to optimize, 2018.
- 379 [13] David Eriksson, Kun Dong, Eric Lee, David Bindel, and Andrew G Wilson. Scaling gaussian
 380 process regression with derivatives. In S. Bengio, H. Wallach, H. Larochelle, K. Grauman, N.
 381 Cesa-Bianchi, and R. Garnett, editors, *Advances in Neural Information Processing Systems 31*,
 382 pages 6867–6877. Curran Associates, Inc., 2018.
- 383 [14] David Eriksson, Michael Pearce, Jacob Gardner, Ryan D Turner, and Matthias Poloczek.
 384 Scalable global optimization via local bayesian optimization. In *Advances in Neural Information*
 385 *Processing Systems 32*, pages 5496–5507. Curran Associates, Inc., 2019.
- 386 [15] Peter I. Frazier. A tutorial on bayesian optimization, 2018.
- 387 [16] Peter I. Frazier, Warren B. Powell, and Savas Dayanik. A knowledge-gradient policy for
 388 sequential information collection. *SIAM J. Control Optim.*, 47(5):2410–2439, Sept. 2008.
- 389 [17] Elad Gilboa, Yunus Saatçi, and John P. Cunningham. Scaling multidimensional Gaussian
 390 processes using projected additive approximations. In *Proceedings of the 30th International*
 391 *Conference on International Conference on Machine Learning - Volume 28*, ICML'13, page
 392 I–454–I–461. JMLR.org, 2013.
- 393 [18] Daniel Golovin, Benjamin Solnik, Subhodeep Moitra, Greg Kochanski, John Karro, and D
 394 Sculley. Google vizier: A service for black-box optimization. In *Proceedings of the 23rd ACM*
 395 *SIGKDD international conference on knowledge discovery and data mining*, pages 1487–1495,
 396 2017.
- 397 [19] Rafael Gómez-Bombarelli, Jennifer N Wei, David Duvenaud, José Miguel Hernández-Lobato,
 398 Benjamín Sánchez-Lengeling, Dennis Sheberla, Jorge Aguilera-Iparraguirre, Timothy D Hirzel,
 399 Ryan P Adams, and Alán Aspuru-Guzik. Automatic chemical design using a data-driven
 400 continuous representation of molecules. *ACS central science*, 4(2):268–276, 2018.
- 401 [20] Javier Gonzalez, Zhenwen Dai, Philipp Hennig, and Neil Lawrence. Batch bayesian optimization
 402 via local penalization. In Arthur Gretton and Christian C. Robert, editors, *Proceedings of the*

- 403 *19th International Conference on Artificial Intelligence and Statistics*, volume 51 of *Proceedings*
404 *of Machine Learning Research*, pages 648–657, Cadiz, Spain, 09–11 May 2016. PMLR.
- 405 [21] Luigi Grippo and Marco Sciandrone. On the convergence of the block nonlinear gauss-seidel
406 method under convex constraints. *Operations Research Letters*, 26(3):127–136, 2000.
- 407 [22] Nikolaus Hansen and Andreas Ostermeier. Completely derandomized self-adaptation in evolu-
408 tion strategies. *Evolutionary Computation*, 9(2):159–195, June 2001.
- 409 [23] David Haussler, Jyrki Kivinen, and Manfred K Warmuth. Tight worst-case loss bounds for
410 predicting with expert advice. In *European Conference on Computational Learning Theory*,
411 pages 69–83. Springer, 1995.
- 412 [24] Philipp Hennig and Christian J. Schuler. Entropy search for information-efficient global
413 optimization. *J. Mach. Learn. Res.*, 13(1):1809–1837, June 2012.
- 414 [25] José Miguel Henrández-Lobato, Matthew W. Hoffman, and Zoubin Ghahramani. Predictive
415 entropy search for efficient global optimization of black-box functions. In *Proceedings of the*
416 *27th International Conference on Neural Information Processing Systems - Volume 1, NIPS’14*,
417 page 918–926, Cambridge, MA, USA, 2014. MIT Press.
- 418 [26] IDW. https://en.wikipedia.org/wiki/Inverse_distance_weighting.
- 419 [27] Donald R. Jones, Matthias Schonlau, and William J. Welch. Efficient global optimization of
420 expensive black-box functions. *Journal of Global optimization*, 13(4):455–492, 1998.
- 421 [28] Kirthevasan Kandasamy, Jeff Schneider, and Barnabás Póczos. High dimensional bayesian
422 optimization and bandits via additive models. In *Proceedings of the 32nd International Confer-*
423 *ence on International Conference on Machine Learning - Volume 37, ICML’15*, page 295–304.
424 JMLR.org, 2015.
- 425 [29] Johannes Kirschner, Mojmir Mutny, Nicole Hiller, Rasmus Ischebeck, and Andreas Krause.
426 Adaptive and safe Bayesian optimization in high dimensions via one-dimensional subspaces. In
427 Kamalika Chaudhuri and Ruslan Salakhutdinov, editors, *Proceedings of the 36th International*
428 *Conference on Machine Learning*, volume 97 of *Proceedings of Machine Learning Research*,
429 pages 3429–3438, Long Beach, California, USA, 09–15 Jun 2019. PMLR.
- 430 [30] H. J. Kushner. A new method of locating the maximum point of an arbitrary multipeak curve in
431 the presence of noise. *Journal of Basic Engineering*, 86(1):97–106, mar 1964.
- 432 [31] Rémi Lam, Matthias Poloczek, Peter Frazier, and Karen E Willcox. Advances in bayesian
433 optimization with applications in aerospace engineering. In *2018 AIAA Non-Deterministic*
434 *Approaches Conference*, page 1656, 2018.
- 435 [32] Ben Letham, Roberto Calandra, Akshara Rai, and Eytan Bakshy. Re-examining linear embed-
436 dings for high-dimensional bayesian optimization. *Advances in Neural Information Processing*
437 *Systems*, 33, 2020.
- 438 [33] Ben Letham, Roberto Calandra, Akshara Rai, and Eytan Bakshy. Re-examining linear embed-
439 dings for high-dimensional bayesian optimization. In H. Larochelle, M. Ranzato, R. Hadsell,
440 M. F. Balcan, and H. Lin, editors, *Advances in Neural Information Processing Systems*, vol-
441 ume 33, pages 1546–1558. Curran Associates, Inc., 2020.
- 442 [34] Benjamin Letham, Brian Karrer, Guilherme Ottoni, Eytan Bakshy, et al. Constrained bayesian
443 optimization with noisy experiments. *Bayesian Analysis*, 14(2):495–519, 2019.
- 444 [35] Cheng Li, Sunil Gupta, Santu Rana, Vu Nguyen, Svetha Venkatesh, and Alistair Shilton.
445 High dimensional bayesian optimization using dropout. In *Proceedings of the Twenty-Sixth*
446 *International Joint Conference on Artificial Intelligence, IJCAI-17*, pages 2096–2102, 2017.
- 447 [36] Chun-Liang Li, Kirthevasan Kandasamy, Barnabas Poczos, and Jeff Schneider. High dimen-
448 sional bayesian optimization via restricted projection pursuit models. In Arthur Gretton and
449 Christian C. Robert, editors, *Proceedings of the 19th International Conference on Artificial*
450 *Intelligence and Statistics*, volume 51 of *Proceedings of Machine Learning Research*, pages
451 884–892, Cadiz, Spain, 09–11 May 2016. PMLR.
- 452 [37] Daniel J Lizotte, Tao Wang, Michael H Bowling, and Dale Schuurmans. Automatic gait
453 optimization with gaussian process regression. In *IJCAI*, volume 7, pages 944–949, 2007.
- 454 [38] LunarLander v2. <https://gym.openai.com/envs/LunarLander-v2/>.
- 455 [39] Horia Mania, Aurelia Guy, and Benjamin Recht. Simple random search of static linear policies
456 is competitive for reinforcement learning. In S. Bengio, H. Wallach, H. Larochelle, K. Grauman,
457 N. Cesa-Bianchi, and R. Garnett, editors, *Advances in Neural Information Processing Systems*
458 *31*, pages 1800–1809. Curran Associates, Inc., 2018.
- 459 [40] Matern kernel. [https://scikit-learn.org/stable/modules/generated/sklearn.](https://scikit-learn.org/stable/modules/generated/sklearn.gaussian_process.kernels.Matern.html)
460 [gaussian_process.kernels.Matern.html](https://scikit-learn.org/stable/modules/generated/sklearn.gaussian_process.kernels.Matern.html).

- 461 [41] Mark McLeod, Michael A. Osborne, and Stephen J. Roberts. Optimization, fast and slow:
462 Optimally switching between local and bayesian optimization. In *ICML*, 2018.
- 463 [42] J. Močkus. On bayesian methods for seeking the extremum. In G. I. Marchuk, editor, *Optimization
464 Techniques IFIP Technical Conference Novosibirsk, July 1–7, 1974*, pages 400–404, Berlin,
465 Heidelberg, 1975. Springer Berlin Heidelberg.
- 466 [43] Riccardo Moriconi, K. S. Sesh Kumar, and Marc Peter Deisenroth. High-dimensional bayesian
467 optimization with projections using quantile gaussian processes. *Optimization Letters*, 14:51–64,
468 2020.
- 469 [44] Alexander Munteanu, Amin Nayebi, and Matthias Poloczek. A framework for Bayesian
470 optimization in embedded subspaces. In Kamalika Chaudhuri and Ruslan Salakhutdinov,
471 editors, *Proceedings of the 36th International Conference on Machine Learning*, volume 97 of
472 *Proceedings of Machine Learning Research*, pages 4752–4761, Long Beach, California, USA,
473 09–15 Jun 2019. PMLR.
- 474 [45] Mojmir Mutny and Andreas Krause. Efficient high dimensional bayesian optimization with
475 additivity and quadrature fourier features. In S. Bengio, H. Wallach, H. Larochelle, K. Grauman,
476 N. Cesa-Bianchi, and R. Garnett, editors, *Advances in Neural Information Processing Systems
477 31*, pages 9005–9016. Curran Associates, Inc., 2018.
- 478 [46] Julie Nutini, Mark Schmidt, Issam H. Laradji, Michael Friedlander, and Hoyt Koepke. Coordinate
479 descent converges faster with the gauss-southwell rule than random selection. *ICML’15:
480 Proceedings of the 32nd International Conference on International Conference on Machine
481 Learning*, 37, July 2015.
- 482 [47] ChangYong Oh, Efstratios Gavves, and Max Welling. BOCK : Bayesian optimization with
483 cylindrical kernels. In Jennifer Dy and Andreas Krause, editors, *Proceedings of the 35th
484 International Conference on Machine Learning*, volume 80 of *Proceedings of Machine Learning
485 Research*, pages 3868–3877, Stockholm, Sweden, 10–15 Jul 2018. PMLR.
- 486 [48] Rafael Oliveira, Fernando Rocha, Lionel Ott, Vitor Guizilini, Fabio Ramos, and Valdir Jr.
487 Learning to race through coordinate descent bayesian optimisation. In *IEEE International
488 Conference on Robotics and Automation (ICRA)*, February 2018.
- 489 [49] M.J.D. Powell. *On Search Directions for Minimization Algorithms*. AERE-TP. AERE, Theoret-
490 ical Physics Division, 1972.
- 491 [50] Radial basis function. [https://docs.scipy.org/doc/scipy/reference/generated/
492 scipy.interpolate.Rbf.html](https://docs.scipy.org/doc/scipy/reference/generated/scipy.interpolate.Rbf.html).
- 493 [51] Ali Rahimi and Benjamin Recht. Random features for large-scale kernel machines. In J. C. Platt,
494 D. Koller, Y. Singer, and S. T. Roweis, editors, *Advances in Neural Information Processing
495 Systems 20*, pages 1177–1184. Curran Associates, Inc., 2008.
- 496 [52] Akshara Rai, Rika Antonova, Seungmoon Song, William Martin, Hartmut Geyer, and Christo-
497 pher Atkeson. Bayesian optimization using domain knowledge on the atrias biped. In *2018
498 IEEE International Conference on Robotics and Automation (ICRA)*, pages 1771–1778. IEEE,
499 2018.
- 500 [53] Warren Scott, Peter Frazier, and Warren Powell. The correlated knowledge gradient for
501 simulation optimization of continuous parameters using gaussian process regression. *SIAM
502 Journal on Optimization*, 21(3):996–1026, 2011.
- 503 [54] Niranjan Srinivas, Andreas Krause, Sham Kakade, and Matthias Seeger. Gaussian process
504 optimization in the bandit setting: No regret and experimental design. In *Proceedings of the
505 27th International Conference on International Conference on Machine Learning*, ICML’10,
506 page 1015–1022, Madison, WI, USA, 2010.
- 507 [55] N. Srinivas, A. Krause, S. M. Kakade, and M. W. Seeger. Information-theoretic regret bounds
508 for gaussian process optimization in the bandit setting. *IEEE Transactions on Information
509 Theory*, 58(5):3250–3265, 2012.
- 510 [56] Rainer Storn and Kenneth Price. Differential evolution—a simple and efficient heuristic for
511 global optimization over continuous spaces. *Journal of global optimization*, 11(4):341–359,
512 1997.
- 513 [57] Sonja Surjanovic and Derek Bingham. Optimization test problems, 2013.
- 514 [58] Hemant Tyagi and Volkan Cevher. Learning non-parametric basis independent models from
515 point queries via low-rank methods. *Applied and Computational Harmonic Analysis*, 37(3):389
516 – 412, 2014.

- 517 [59] Emmanuel Vazquez and Julien Bect. Convergence properties of the expected improvement
518 algorithm with fixed mean and covariance functions. *Journal of Statistical Planning and*
519 *Inference*, 140(11):3088 – 3095, 2010.
- 520 [60] Linnan Wang, Rodrigo Fonseca, and Yuandong Tian. Learning search space partition for
521 black-box optimization using monte carlo tree search. *ArXiv*, abs/2007.00708, 2020.
- 522 [61] Zi Wang, Clement Gehring, Pushmeet Kohli, and Stefanie Jegelka. Batched large-scale bayesian
523 optimization in high-dimensional spaces. In *International Conference on Artificial Intelligence*
524 *and Statistics (AISTATS)*, 2018.
- 525 [62] Zi Wang, Clement Gehring, Pushmeet Kohli, and Stefanie Jegelka. Batched large-scale bayesian
526 optimization in high-dimensional spaces. In *International Conference on Artificial Intelligence*
527 *and Statistics*, pages 745–754, 2018.
- 528 [63] Ziyu Wang, Frank Hutter, Masrour Zoghi, David Matheson, and Nando De Freitas. Bayesian
529 optimization in a billion dimensions via random embeddings. *J. Artif. Int. Res.*, 55(1):361–387,
530 Jan. 2016.
- 531 [64] Zi Wang and Stefanie Jegelka. Max-value entropy search for efficient Bayesian optimization. In
532 Doina Precup and Yee Whye Teh, editors, *Proceedings of the 34th International Conference on*
533 *Machine Learning*, volume 70 of *Proceedings of Machine Learning Research*, pages 3627–3635,
534 International Convention Centre, Sydney, Australia, 06–11 Aug 2017. PMLR.
- 535 [65] Zi Wang, Chengtao Li, Stefanie Jegelka, and Pushmeet Kohli. Batched high-dimensional
536 bayesian optimization via structural kernel learning. In *Proceedings of the 34th International*
537 *Conference on Machine Learning - Volume 70*, ICML’17, page 3656–3664. JMLR.org, 2017.
- 538 [66] Ziyu Wang, Masrour Zoghi, Frank Hutter, David Matheson, and Nando De Freitas. Bayesian
539 optimization in high dimensions via random embeddings. In *Proceedings of the Twenty-Third*
540 *International Joint Conference on Artificial Intelligence*, IJCAI ’13, page 1778–1784. AAAI
541 Press, 2013.
- 542 [67] J. Warga. Minimizing certain convex functions. *Journal of the Society for Industrial and*
543 *Applied Mathematics*, 11(3):588–593, 1963.
- 544 [68] Stephen J. Wright. Coordinate descent algorithms. *Mathematical Programming: Series A and*
545 *B*, June 2015.
- 546 [69] Jian Wu and Peter I. Frazier. The parallel knowledge gradient method for batch bayesian
547 optimization. In *Proceedings of the 30th International Conference on Neural Information*
548 *Processing Systems*, NIPS’16, page 3134–3142, Red Hook, NY, USA, 2016. Curran Associates
549 Inc.
- 550 [70] Miao Zhang, Huiqi Li, and Steven Su. High dimensional bayesian optimization via supervised
551 dimension reduction. In *Proceedings of the Twenty-Eighth International Joint Conference on*
552 *Artificial Intelligence*, IJCAI-19, pages 4292–4298. International Joint Conferences on Artificial
553 Intelligence Organization, 7 2019.
- 554 [71] Yichi Zhang, Daniel W Apley, and Wei Chen. Bayesian optimization for materials design with
555 mixed quantitative and qualitative variables. *Scientific reports*, 10(1):1–13, 2020.

556 **Broader Impact**

557 As stated in [32], Bayesian optimization is a powerful optimization technique used in a wide range of
558 industries and applications, such as robotics [37, 9, 52], internet tech companies [18, 34], designing
559 novel molecules for pharmaceuticals [19], material design for increasing efficiency of solar cells [71],
560 and aerospace engineering [31]. All of these settings have high-dimensional optimization problems,
561 and advances in BO will reflect on improved capabilities on these fields as well. We have fully open-
562 sourced our code for CobBO using the MIT license to be available for researchers and practitioners
563 in these fields, and many others. The ability to optimize a larger number of parameters than has
564 previously been possible will bring further improvements to and further accelerate work in these
565 areas.

566 **Checklist**

567 The checklist follows the references. Please read the checklist guidelines carefully for information on
568 how to answer these questions. For each question, change the default **[TODO]** to **[Yes]**, **[No]**, or

569 [N/A] . You are strongly encouraged to include a **justification to your answer**, either by referencing
570 the appropriate section of your paper or providing a brief inline description. For example:

- 571 • Did you include the license to the code and datasets? [Yes] See Section ??.
- 572 • Did you include the license to the code and datasets? [No] The code and the data are
573 proprietary.
- 574 • Did you include the license to the code and datasets? [N/A]

575 Please do not modify the questions and only use the provided macros for your answers. Note that the
576 Checklist section does not count towards the page limit. In your paper, please delete this instructions
577 block and only keep the Checklist section heading above along with the questions/answers below.

578 1. For all authors...

- 579 (a) Do the main claims made in the abstract and introduction accurately reflect the paper's
580 contributions and scope? [Yes] See Section 3.
- 581 (b) Did you describe the limitations of your work? [No]
- 582 (c) Did you discuss any potential negative societal impacts of your work? [Yes] See
583 Broader Impact.
- 584 (d) Have you read the ethics review guidelines and ensured that your paper conforms to
585 them? [Yes]

586 2. If you are including theoretical results...

- 587 (a) Did you state the full set of assumptions of all theoretical results? [Yes] See Section 3.3.
- 588 (b) Did you include complete proofs of all theoretical results? [Yes] See the Appendix A.

589 3. If you ran experiments...

- 590 (a) Did you include the code, data, and instructions needed to reproduce the main ex-
591 perimental results (either in the supplemental material or as a URL)? [Yes] In the
592 supplemental material.
- 593 (b) Did you specify all the training details (e.g., data splits, hyperparameters, how they
594 were chosen)? [Yes] See Table 2 in the appendix, which contains the default hyperpa-
595 rameters.
- 596 (c) Did you report error bars (e.g., with respect to the random seed after running experi-
597 ments multiple times)? [Yes] See Fig.5 and Fig.8-10.
- 598 (d) Did you include the total amount of compute and the type of resources used (e.g., type
599 of GPUs, internal cluster, or cloud provider)? [Yes] See page 9, line 324.

600 4. If you are using existing assets (e.g., code, data, models) or curating/releasing new assets...

- 601 (a) If your work uses existing assets, did you cite the creators? [N/A]
- 602 (b) Did you mention the license of the assets? [Yes] MIT license; see the appendix.
- 603 (c) Did you include any new assets either in the supplemental material or as a URL? [No]
- 604 (d) Did you discuss whether and how consent was obtained from people whose data you're
605 using/curating? [Yes] See Section 4.2.
- 606 (e) Did you discuss whether the data you are using/curating contains personally identifiable
607 information or offensive content? [N/A] It does not contain personal identifiable
608 information or offensive content.

609 5. If you used crowdsourcing or conducted research with human subjects...

- 610 (a) Did you include the full text of instructions given to participants and screenshots, if
611 applicable? [N/A]
- 612 (b) Did you describe any potential participant risks, with links to Institutional Review
613 Board (IRB) approvals, if applicable? [N/A]
- 614 (c) Did you include the estimated hourly wage paid to participants and the total amount
615 spent on participant compensation? [N/A]